

A photoexcited wideband silicon-based tunable metamaterial absorber with wide-angle absorption for terahertz waves

LIANSHENG WANG^{a,*}, DONGYAN XIA^b, QUANHONG FU^c, XUEYONG DING^a, YUAN WANG^a

^aScience and Technology Department, Sanya University, Sanya, Hainan, 572022, China

^bFinance and Economics Department, Sanya University, Sanya, Hainan, 572022, China

^cScience Department, Northwestern Polytechnical University, Xi'an, Shanxi, 710072, China

We design a new kind of metamaterial absorber in the form of photoconductive silicon disk capable of having tunable wideband absorption of terahertz waves. We demonstrate the absorption of absorber reach up to 90% within the entire frequency band of 4THz–6.5THz when the conductivity of silicon is 5000S/m, and it process the tunable property by alter the photoexcited conductivity of silicon disk. Moreover, we study the electric and magnetic fields distribution at some frequency within the absorption band in order to analysis the wideband absorption mechanism. Finally, we prove that the absorber has the property of polarization-insensitive and wide-angle absorption for terahertz waves. The proposed metamaterial absorber is low-cost, easy to prepare, and useful for terahertz waves modulation and switching.

(Received August 11, 2019; accepted August 18, 2020)

Keywords: Wideband, Tunable, Metamaterial absorber, Terahertz waves

1. Introduction

Metamaterials (MMs) is a new kind of artificially composite material composed of sub-wavelength periodic structures. Over past decades, the research of MMs have attracted great attentions due to its property not available in nature [1-3] and many functional MMs has be demonstrated from microwave band to visible regime [4-10]. The research of MMs in terahertz (THz) MMs as a potential solution to construct high performance THz devices is especially important due to the lack of natural material to response the THz waves [11]. Metamaterial absorber in THz regime has the potential application in switcher, modulator, detection, sensing, and so on [12,13].

Over the past years, many wideband MMA in THz regime is fabricated and theoretically analyzed using a variety of designed configurations. In 2015, Li et al. [14] proposed a wideband MMA consisting of multi-layer square resistive surfaces with different sizes, its absorption is over 90% form 2.6 THz to 5.7 THz. In 2016, Wu et al. [15] proposed a wideband MMA consisting of multi-layer metal and dielectric, its absorption is over 90% from 1.666 THz to 2.562 THz. In 2018, Rahmzadeh et al. [16] proposed a wideband MMA consisting of square, cross and circular graphene metal surfaces embedded three layers dielectrics, its absorption is over 90% from 0.55 THz to 3.12 THz. However, the above mentioned wideband MMA in THz regime are all multi-layer, which not only increases the processing difficulty, but also limits

their applications in some fields.

In this work, we present a new kind of metamaterial absorber in the form of photoconductive silicon disk capable of having tunable wideband absorption of terahertz waves. We demonstrate the absorption of absorber reach up to 90% within the entire frequency band of 4THz~6.5THz when the conductivity of silicon is 7000S/m, and it process the tunable property by alter the external pump power applied on silicon disk. The proposed metamaterial absorber is low-cost, easy to prepare, and useful for terahertz waves modulation and switching.

2. Design theory

The equivalent circuit of MMA based on resistive film is shown in Fig. 1. According to the theory of transmission line, the input impedance of MMA based on resistive film

can be expressed as
$$Z_{in} = \frac{1}{1/Z_p + 1/Z_d} = \frac{Z_p Z_d}{Z_p + Z_d}$$
 (Z_d

is dielectric impedance, Z_p is the surface impedance).

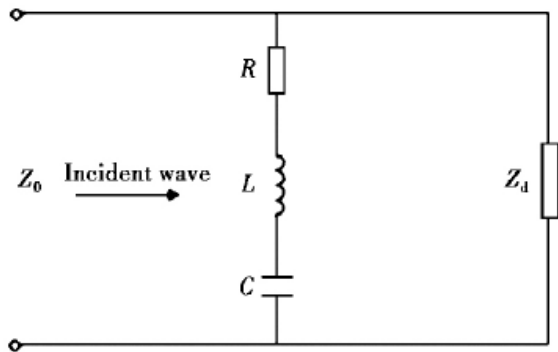


Fig. 1. The equivalent circuit diagram of metamaterial absorber based on resistive film

The dielectric impedance Z_d can be expressed as [17]:

$$Z_d = jZ_0 \sqrt{\frac{1}{\epsilon_r}} \tan(\omega d \sqrt{\epsilon_0 \epsilon_r \mu_0}) \quad (1)$$

In the formula (1), Z_0 is the impedance of free space, ϵ_0 and μ_0 is the permittivity and permeability of free space, ω is the resonant angular frequency, d is the thickness of dielectric layer and ϵ_r is the relative permittivity of dielectric layer.

The surface impedance Z_p can be expressed as

[18]:

$$Z_p = \frac{S_{unitcell}}{S_{patch}} R_s + j\omega L - 1/(j\omega C) \quad (2)$$

In the formula (2), R_s is the sheet resistance of resistive film, $S_{unitcell}$ and S_{patch} are the area of unit cell and resistive film. We can see from formula (1) and (2) that the absorption of MMA based on resistive film can be tuned by alter the sheet resistance of resistive film. At the same time, the MMA based on resistive film can realize wideband absorption due to the produced heat loss of resistive film under the action of incident electromagnetic wave.

The conductivity of silicon in THz regime can be tuned via photo-excitation [19,20], so the tunable wideband MMA in The regime can be realized using silicon as the resistive film.

3. Model design

Our MMA is composed of a silicon disk array above a conductive ground plane layer separated with a dielectric substrate, as Fig. 1. The silicon disk is simulated as a dielectric with permittivity of $\epsilon_r = 11.7$ and pump

power-dependent conductivity [19,20], its geometric parameters are as follows: $r = 6\mu m$, $t = 1\mu m$. The dielectric substrate is composed of polyimide with $\epsilon_r = 2.88$ and $\tan \delta = 0.0313$ in THz regime [21], its geometric parameters are as follows: $a = b = 6\mu m$, $h = 6\mu m$. The conductive ground plane layer is made of gold with conductivity $\sigma = 4.09 \times 10^7 S/m$ [21], its thickness is $g = 0.2\mu m$. All the above mentioned parameters are obtained by parameter optimization.

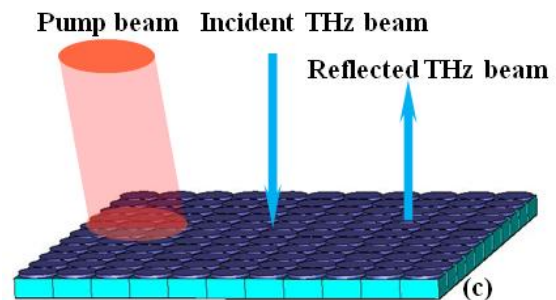
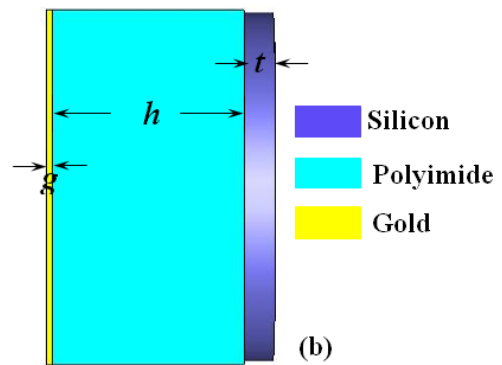
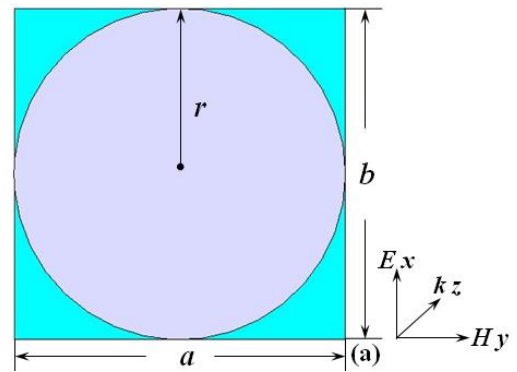


Fig. 2. Scheme of the proposed MMA, (a and b) the unit cell structure, (c) two-dimensional array (color online)

The modeling and numerical simulation of our MMA is performed with Microwave Studio CST. At the simulation process, the boundary condition of x and y directions are set as unit cell, the z direction is set as open, the All+Floquet ports is used to simulating the incoming and outgoing waves. The electromagnetic parameters are calculated by using frequency domain electromagnetic solver.

4. Results and discussion

As the copper substrate of unit cell prevents the incident wave penetrating, the transmittance

$T(\omega) = |S_{12}|^2 = 0$, the absorption can be calculated by

$A(\omega) = 1 - |S_{11}|^2 - |S_{21}|^2 = 1 - |S_{11}|^2$. Fig. 3 shows the

simulated absorption for different silicon conductivities. It can be seen from Fig. 3 that the absorption reach its maximum when the conductivity of silicon is 5000 S/m, and the frequency with the absorption over 90% is from 4 THz to 6 THz. The absorption gradually decreases with the decreasing of the conductivity. By using the definitions of the strength modulation depth

$$M = \frac{|A_{bias} - A_{max}|}{A_{max}} \times 100\% \quad (A_{bias} \text{ is the absorption of MMA at different conductivity of silicon, } A_{max} \text{ is the maximal absorption of MMA) [19],$$

the corresponding modulation depth is up to 70%. The reason of tunable absorption is that the surface impedance Z_p of MMA will decrease with the increasing of the conductivity of silicon according to the formula (2), this will dent the impedance match of MMA with free space, and then lead to the deceasing of absorption with the increasing of the conductivity of silicon.

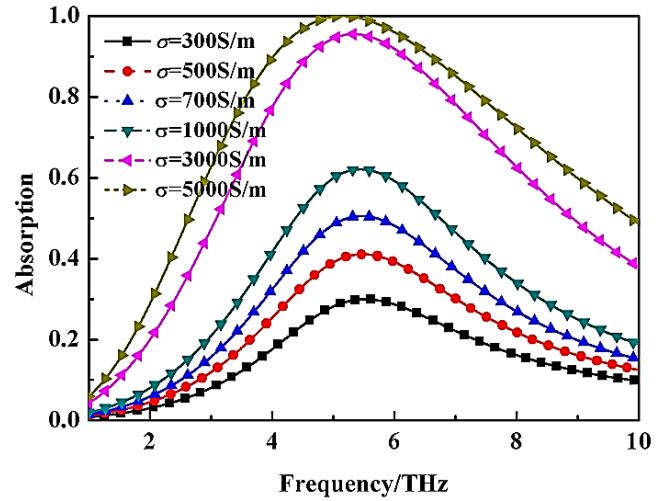


Fig. 3. The absorption of the proposed MMA with different silicon conductivity (color online)

According to the calculation formula of absorption

$$A(\omega) = 1 - R(\omega) = 1 - \left| \frac{Z(\omega) - Z_0}{Z(\omega) + Z_0} \right|^2, \quad \text{the perfect}$$

absorption of incident wave is achieved when the input impedance of MMA is equal to free space. According to the S parameters extracted by simulation, the normalized impedance ($Z(\omega)/Z_0$) under perpendicular incident wave when the conductivity of silicon is 5000 S/m calculated by scattering parameter method (the distance of input port with MMA is $3 \mu\text{m}$) [22], the result is shown in Fig. 4. We can see from Fig. 4 that the normalized impedance of MMA with free space from 4 THz to 6 THz is close to one, it indicates that a well acceptable impedance match of MMA with free space is accomplished, as an outcome the perfect absorption can be realized in this case.

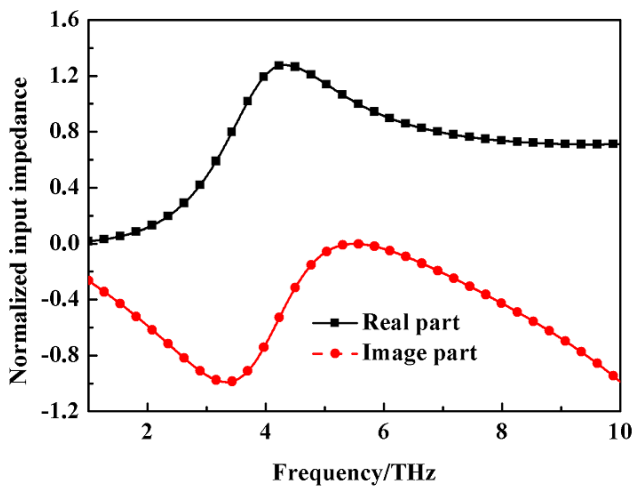


Fig. 4. The normalized input impedance of absorber with free space when the conductivity of silicon is 5000 S/m under perpendicular incident wave (color online)

In order to better understand the physical mechanism of wideband absorption, the electric and magnetic field distributions are numerically investigated at 4THz, 5THz and 6THz, as shown in Fig. 5. We see from Fig. 5 that the electric field mainly concentrates on the upper left and upper right part of unit cell and the magnetic field mainly concentrates on the middle part of silicon disk at 4THz and 5THz. This indicates that there are both strong electrical and magnetic resonances at these frequencies [8]. For 6THz, the magnetic field is mainly concentrated on the middle part of silicon disk and the bottom part of polyimide, but the electric field is significantly weaker, indicating that the main role is a strong magnetic resonance and the electric resonance is much weaker at 6THz [8]. These resonances in the metamaterial are close to each other in frequency, which are merged together to form a wideband absorption.

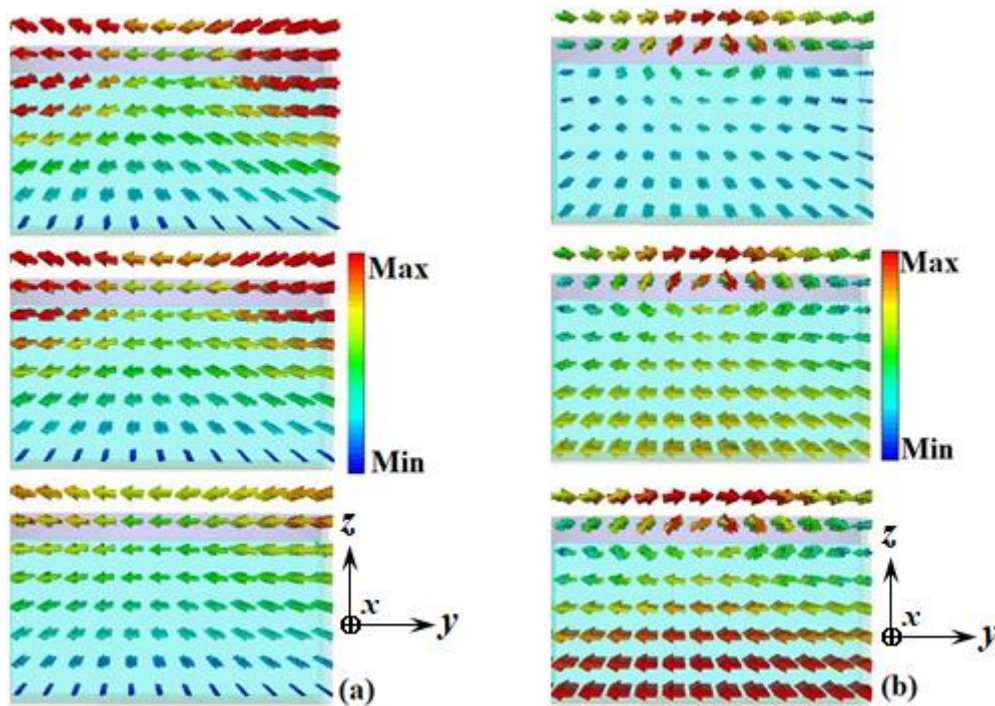


Fig. 5. Vector distributions of (a) electric and (b) magnetic fields at resonance frequencies: 4 THz (top), 5 THz (middle), and 6THz (bottom) (color online)

For a better illustration of the absorption of MMA, the power loss densities at the 4 THz, 5 THz and 6 THz are further shown in Fig. 6. It shows that, in all cases, the power loss densities mainly concentrate on the polyimide layer, which is simply due to the high dielectric loss of polyimide over the frequency range of interest.

The above results are calculated at the condition of THz wave incident vertically on MMA, but the practical application requires MMA to have high absorption at wide

range of incident angle and different polarization. Therefore, the absorption of MMA at different polarization and incident angle are simulated (the conductivity of silicon is 5000 S/m), the results are shown in Fig. 7 and Fig. 8. It can be seen from Fig. 7 that the absorption of MMA is insensitive to polarization because of the rotational symmetry of unit cell. It is noticeable in Fig. 8 that the absorption of MMA gradually decreases with the increasing of incident angle from 0° to 80° at TE and TM

mode, but the absorption is still up to 70% from 4THz to 6.5 THz at the incident angle of 60°.

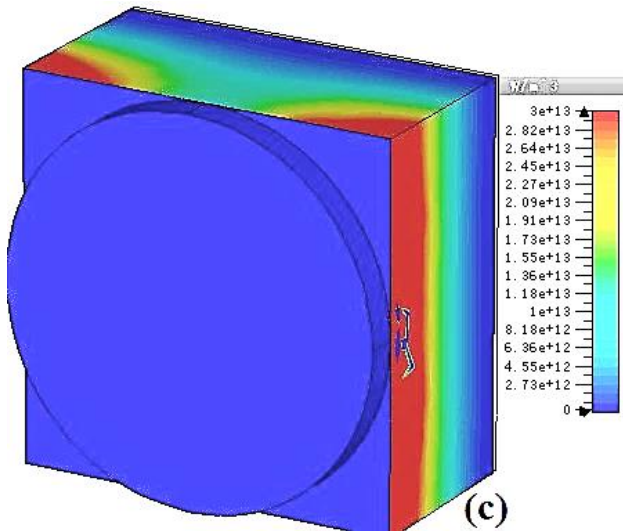
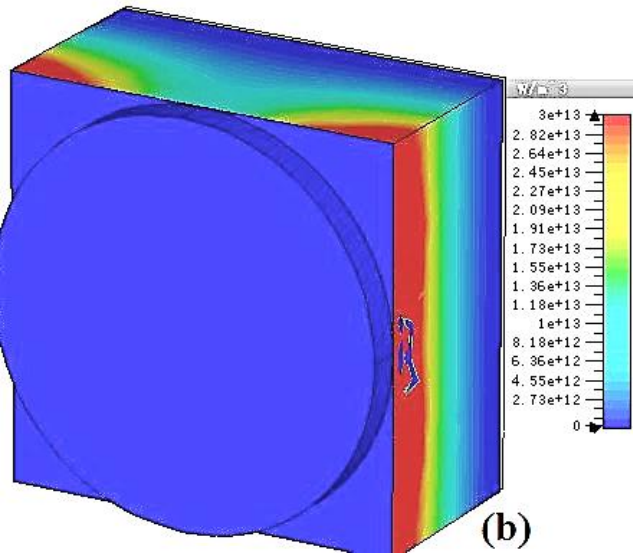
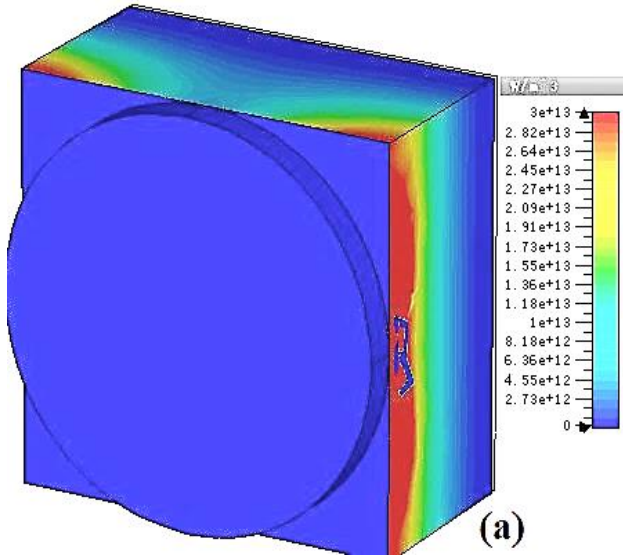


Fig. 6. The power loss densities of MMA at (a) 4THz, (b) 5THz and at (c) 6THz (color online)

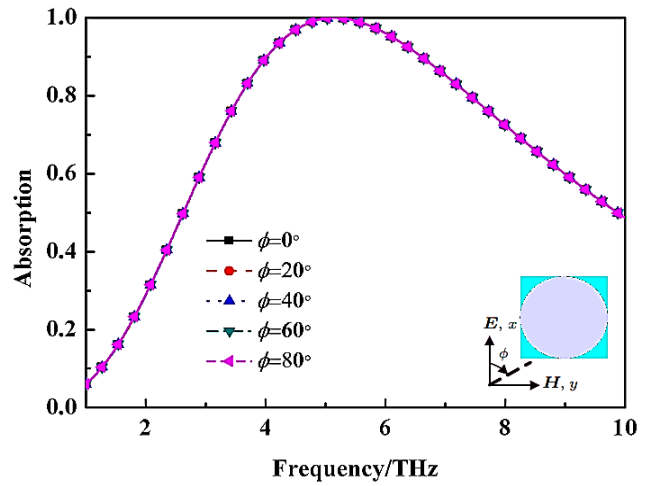


Fig. 7. The absorption of absorber at different polarization angle when the conductivity of silicon is 5000S/m under perpendicular incident wave (color online)

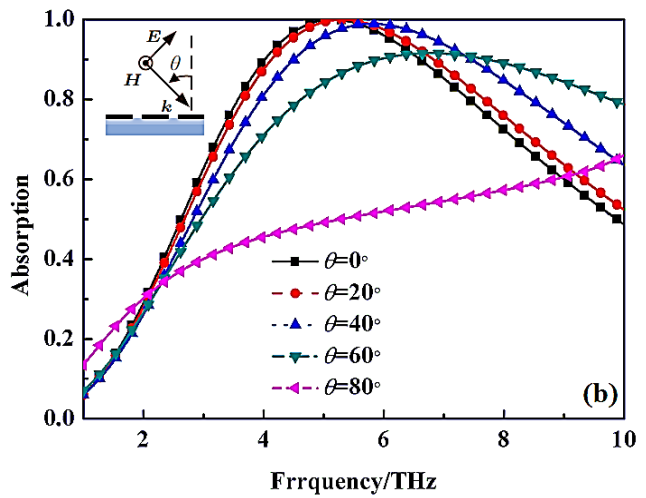
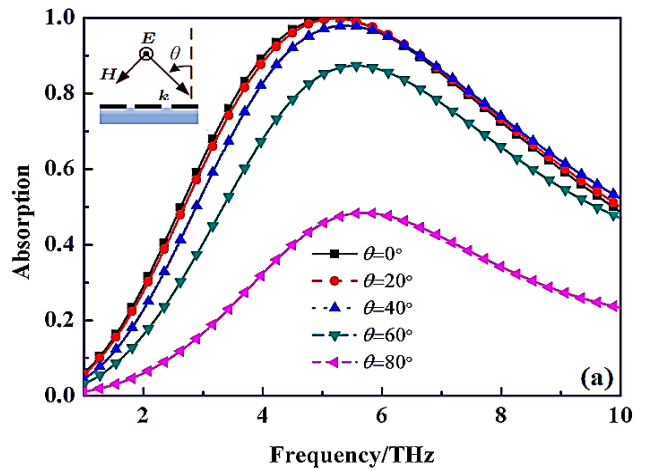


Fig. 8. The absorption of absorber at different incident angle when the conductivity of silicon is 5000 S/m, (a) TE mode; (b)TM mode (color online)

Finally, the effect of geometric parameter r and t on the absorption when the conductivity of silicon is 5000 S/m is investigated, the results are shown in Fig. 9 and Fig. 9. We can see from Fig. 9 that the absorption of MMA gradually decrease with the decreasing of r and t . The main reason is that the resistance of silicon disk gradually decrease with the decreasing of r and t , this lead to the impedance match of MMA with free space decrease.

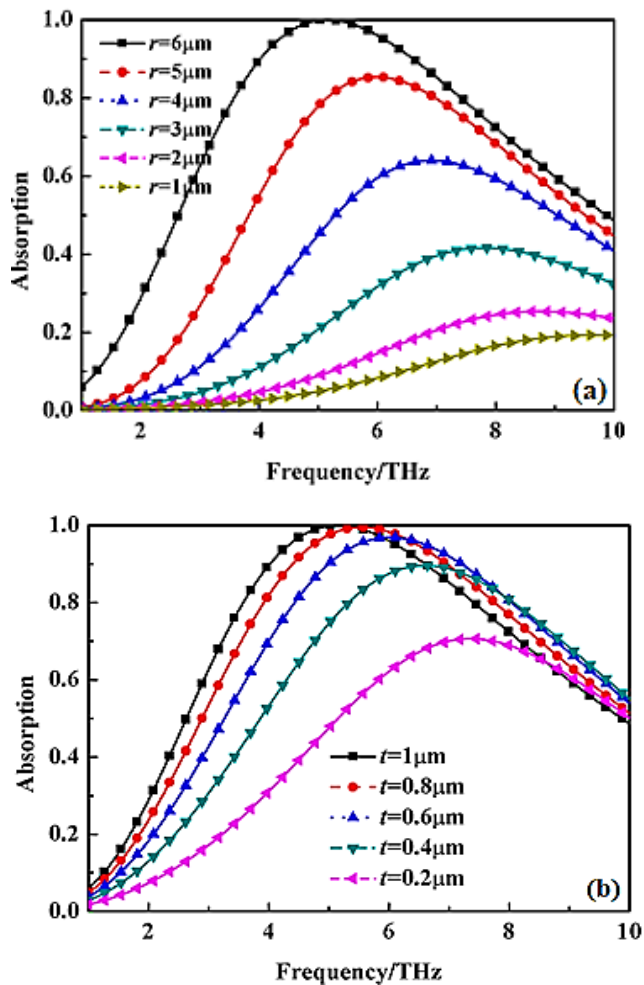


Fig. 9. The absorption of absorber at different geometric parameters when the conductivity of silicon is 5000 S/m under perpendicular incident wave, (a) different geometric parameter r , (b) different geometric parameter t (color online)

5. Conclusion

We present a new kind of MMA in the form of photoconductive silicon disk capable of having tunable wideband absorption of terahertz waves. Firstly, the absorption of MMA at different conductivity of silicon is calculated using Microwave Studio CST, the results show that the absorption of absorber reach up to 90% within the entire frequency band of 4 THz ~ 6.5 THz when the conductivity of silicon is 5000 S/m, and the absorption decrease with the decreasing of photoexcited conductivity of silicon. Moreover, the resonance induced electric field and magnetic field distribution are discussed at different

frequencies for investigating the mechanism of the wideband absorption, which also confirms that the incident wave energies are mainly consumed in the structured polyimide layer. Finally, the absorption of MMA at different polarization and incident angle are studied, which demonstrate that the absorber has the property of polarization-insensitive and wide-angle absorption for terahertz waves. The proposed metamaterial absorber is low-cost, easy to prepare, and useful for terahertz waves modulation and switching.

References

- [1] R. A. Shelby, D. R. Smith, S. Schultz, *Science* **292**, 77 (2001).
- [2] W. Cai, V. Shalaev, *Optical metamaterials: fundamentals and applications*, Springer, New York, (2010).
- [3] T. J. Cui, R. S. David, R. Liu, *Metamaterials: Theory, Design and Applications* Springer, New York, (2010).
- [4] D. Schurig, J. J. Mock, B. J. Justice et al., *Science* **314**, 977 (2006).
- [5] J. Yang, C. Sauvan, H. T. Liu et al., *Phys. Rev. Lett.* **107**, 043903 (2011).
- [6] W. R. Zhu, I. D. Rukhlenko, F. J. Xiao et al., *Opt. Express* **25**(14), 15737 (2017).
- [7] W. R. Zhu, F. J. Xiao, I. D. Rukhlenko et al., *Opt. Express* **25**(5), 5781 (2017).
- [8] J. W. Xie, W. R. Zhu, I. D. Rukhlenko et al., *Opt. Express* **26**(4), 5052 (2018).
- [9] J. W. Xie, S. Quader, F. J. Xiao et al., *IEEE Antennas Wireless Propag. Lett.* **18**(3), 536 (2019).
- [10] M. R. Akram, M. Q. Mehmood, T. Tauqeer et al., *Optics Express* **27**(7), 9467 (2009).
- [11] B. Ferguson, X. C. Zhang, *Nat. Mater* **1**, 26 (2002).
- [12] Y. Z. Cheng, W. Withayachumnankul, A. Upadhyay et al., *Adv. Opt. Mater.* **3**, 376 (2015).
- [13] K. Iwaszczuk, A. C. Strikwerda, K. Fan et al., *Opt. Express* **20**, 635 (2012).
- [14] X. W. Li, H. J. Liu, Q. B. Sun et al., *Photon. Nanostruct: Fundam. Appl.* **15**, 81 (2015).
- [15] W. Pan, X. Yu, J. Zhang et al., *IEEE. Photonics Technol. Lett.* **28**, 2335 (2016).
- [16] M. Rahmzadeh, H. Rajabalipanah, A. Abdolali, *Appl. Opt.* **57**, 959 (2018).
- [17] H. T. Chen, *Frontiers of Optoelectronics* **8**(1), 27 (2015).
- [18] Y. Shen, J. Q. Zhang, Y. Q. Pang et al., *Sci. Rep.* **8**, 4423 (2018).
- [19] X. Shen, T. J. Cui, *J. Opt.* **14**, 114012 (2012).
- [20] H. R. Seren, G. R. Keiser, L. Cao et al., *Adv. Opt. Mater.* **2**, 1221 (2014).
- [21] T. Hu, C. M. Bingham, A. C. Strikwerda et al., *Phys. Rev. B* **78**, 241103(R) (2008).
- [22] D. R. Smith, S. Schultz, *Phys. Rev. B* **65**, 195104 (2002).

*Corresponding author: wlswws1982@126.com